Unclassified **NEA/CSNI/R(2000)6/VOL1**

Organisation de Coopération et de Développement Economiques
Organisation for Economic Co-operation and Development

OLIS : 03-Apr-2000
Dist. : 04-Apr-2000

English text only

NUCLEAR ENERGY AGENCY
COMMITTEE ON THE SAFETY OF NUCLEAR INSTALLATIONS

NEA/CSNI/R(2000)6/VOL1
Unclassified

INTERNATIONAL STANDARD PROBLEM (ISP) NO. 41

CONTAINMENT IODINE COMPUTER CODE EXERCISE BASED ON A RADIOIODINE TEST FACILITY (RTF) EXPERIMENT

English text only

89500

Document complet disponible sur OLIS dans son format d'origine
Complete document available on OLIS in its original format

Coordinators:	J. Clara Wren	AECL (Canada)
	Jacques Royen	OECD/NEA
Compiled by:	Joanne Ball	AECL (Canada)
Contributors:	Joanne Ball	AECL (Canada)
	Glenn Glowa	AECL (Canada)
	J. Clara Wren	AECL (Canada)
	Adolf Rydl	NRIR (Czech Republic)
	Christian Poletiko	IPSN (France)
	Yann Billarand	IPSN (France)
	Falk Ewig	GRS, Köln (Germany)
	Friedhelm Funke	Siemens/KWU (Germany)
	Peter Zeh	Siemens/KWU (Germany)
	Akihide Hidaka	JAERI (Japan)
	Randall Gauntt	Sandia (USA)
	Mike Young	Sandia (USA)
	Robin Cripps	PSI (Switzerland)
	Berta Herrero	CIEMAT (Spain)

ORGANISATION FOR ECONOMIC CO-OPERATION AND DEVELOPMENT

Pursuant to Article 1 of the Convention signed in Paris on 14th December 1960, and which came into force on 30th September 1961, the Organisation for Economic Co-operation and Development (OECD) shall promote policies designed:

- to achieve the highest sustainable economic growth and employment and a rising standard of living in Member countries, while maintaining financial stability, and thus to contribute to the development of the world economy;
- to contribute to sound economic expansion in Member as well as non-member countries in the process of economic development; and
- to contribute to the expansion of world trade on a multilateral, non-discriminatory basis in accordance with international obligations.

The original Member countries of the OECD are Austria, Belgium, Canada, Denmark, France, Germany, Greece, Iceland, Ireland, Italy, Luxembourg, the Netherlands, Norway, Portugal, Spain, Sweden, Switzerland, Turkey, the United Kingdom and the United States. The following countries became Members subsequently through accession at the dates indicated hereafter: Japan (28th April 1964), Finland (28th January 1969), Australia (7th June 1971), New Zealand (29th May 1973), Mexico (18th May 1994), the Czech Republic (21st December 1995), Hungary (7th May 1996), Poland (22nd November 1996) and the Republic of Korea (12th December 1996). The Commission of the European Communities takes part in the work of the OECD (Article 13 of the OECD Convention).

NUCLEAR ENERGY AGENCY

The OECD Nuclear Energy Agency (NEA) was established on 1st February 1958 under the name of the OEEC European Nuclear Energy Agency. It received its present designation on 20th April 1972, when Japan became its first non-European full Member. NEA membership today consists of 27 OECD Member countries: Australia, Austria, Belgium, Canada, Czech Republic, Denmark, Finland, France, Germany, Greece, Hungary, Iceland, Ireland, Italy, Japan, Luxembourg, Mexico, the Netherlands, Norway, Portugal, Republic of Korea, Spain, Sweden, Switzerland, Turkey, the United Kingdom and the United States. The Commission of the European Communities also takes part in the work of the Agency.

The mission of the NEA is:

- to assist its Member countries in maintaining and further developing, through international co-operation, the scientific, technological and legal bases required for a safe, environmentally friendly and economical use of nuclear energy for peaceful purposes, as well as
- to provide authoritative assessments and to forge common understandings on key issues, as input to government decisions on nuclear energy policy and to broader OECD policy analyses in areas such as energy and sustainable development.

Specific areas of competence of the NEA include safety and regulation of nuclear activities, radioactive waste management, radiological protection, nuclear science, economic and technical analyses of the nuclear fuel cycle, nuclear law and liability, and public information. The NEA Data Bank provides nuclear data and computer program services for participating countries.

In these and related tasks, the NEA works in close collaboration with the International Atomic Energy Agency in Vienna, with which it has a Co-operation Agreement, as well as with other international organisations in the nuclear field.

CSNI

The NEA Committee on the Safety of Nuclear Installations (CSNI) is an international committee made up of senior scientists and engineers, with broad responsibilities for safety technology and research programmes, and representatives from regulatory authorities. It was set up in 1973 to develop and co-ordinate the activities of the NEA concerning the technical aspects of the design, construction and operation of nuclear installations insofar as they affect the safety of such installations. The Committee's purpose is to foster international co-operation in nuclear safety amongst the OECD Member countries. CSNI's main tasks are to exchange technical information and to promote collaboration between research, development, engineering and regulation organisations; to review the state of knowledge on selected topics of nuclear safety technology and safety assessments, including operating experience; to initiate and conduct programmes to overcome discrepancies, develop improvements and reach consensus on technical issues; to promote co-ordination of work, including the establishment of joint undertakings.

PWG4

CSNI's Principal Working Group on the Confinement of Accidental Radioactive Releases (PWG4) has been given two tasks: containment protection, and fission product retention. Its role is to exchange information on national and international activities in the areas of severe accident phenomena in the containment, fission product phenomena in the primary circuit and the containment, and containment aspects of severe accident management. PWG4 discusses technical issues/reports and their implications, and the results of International Standard Problem (ISP) exercises and specialist meetings, and submits conclusions to the CSNI. It prepares Technical Opinion Papers on major issues. It reviews the main orientations, future trends, emerging issues, co-ordination and interface with other groups in the field of confinement of accidental radioactive releases, identifies necessary activities, and proposes a programme of work to the CSNI.

FPC

The Task Group on Fission Product Phenomena in the Primary Circuit and the Containment (FPC) is a specialised extension of PWG4. Its main tasks are to exchange information, discuss results and programmes, write state-of-the-art reports, organise specialist workshops, perform ISPs in the field of fission product phenomenology.

TABLE OF CONTENTS

1. INTRODUCTION

International Standard Problem (ISP) exercises are comparative exercises in which predictions of different computer codes for a given physical problem are compared with each other or with the results of a carefully controlled experimental study. The main goal of ISP exercises is to increase confidence in the validity and accuracy of the tools, which were used in assessing the safety of nuclear installations. Moreover, they enable code users to gain experience and demonstrate their competence. The ISP No. 41 exercise, computer code exercise based on a Radioiodine Test Facility (RTF) experiment on iodine behaviour in containment under severe accident conditions, is one of such ISP exercises.

The ISP No. 41 exercise was borne at the recommendation at the Fourth Iodine Chemistry Workshop held at PSI, Switzerland in June 1996: *'the performance of an International Standard Problem as the basis of an in-depth comparison of the models as well as contributing to the database for validation of iodine codes.'* [Proceedings NEA/CSNI/R(96)6, Summary and Conclusions NEA/CSNI/R(96)7]. COG (CANDU Owners Group), comprising AECL and the Canadian nuclear utilities, offered to make the results of a Radioiodine Test Facility (RTF) test available for such an exercise. The ISP No. 41 exercise was endorsed in turn by the FPC (PWG4's Task Group on Fission Product Phenomena in the Primary Circuit and the Containment), PWG4 (CSNI Principal Working Group on the Confinement of Accidental Radioactive Releases), and the CSNI. The OECD/NEA Committee on the Safety of Nuclear Installations (CSNI) has sponsored forty-five ISP exercises over the last twenty-four years, thirteen of them in the area of severe accidents.

The criteria for the selection of the RTF test as a basis for the ISP-41 exercise were; (1) complementary to other RTF tests available through the PHEBUS and ACE programmes, (2) simplicity for ease of modelling and (3) good quality data. A simple RTF experiment performed under controlled and very limited conditions was chosen as a starting point for evaluation of the various iodine behaviour codes in the hope that the very basic components of each code could be compared. The experiment was ideal for demonstrating the ability of all of the codes to model the pH behaviour of iodine volatility, one of the most important aspects of iodine behaviour.

The RTF test was conducted in a stainless steel vessel at 25^{o}C and at a dose rate of 1.4 kGy·h^{-1}. The test, which started with about 1 $\times 10^{-5}$ mol·dm^{-3} CsI in the aqueous phase, was conducted in two stages. In both stages, the initial pH was 10, followed by multiple, and controlled, stepwise decreases in pH (to 7.2 in stage 1 and to 5.5 in stage 2). At the end of stage 1, the initial charge solution was discarded, the vessel was rinsed repeatedly to remove adsorbed iodine and a fresh solution of CsI was added to commence stage 2.

The countries (organisations) which took part in the exercise were Canada (AECL), the Czech Republic (NRIR), France (IPSN), Germany (Siemens, GRS), Japan (JAERI), USA (Sandia), Spain (CIEMAT) and Switzerland (PSI). The Canadian team supplied to the participants the details of the experimental set-up, conditions and procedures of the RTF test, including:

- dimensions/volumes/geometric surface areas of vessel and loops;
- pH data measured on line as a function of time;
- dissolved oxygen concentration data (ppm) as a function of time;
- gas and aqueous loop recirculation rates (litres per minute) as a function of time ;

- aqueous and gas phase volumes in the RTF;
- areas of surfaces exposed to the gas and aqueous phase;
- area of the gas/aqueous interface;
- average dose rate in the gas phase and aqueous phase;
- quantity of total iodine added to the RTF;
- initial iodine concentration;
- initial iodine speciation;
- temperature data.

The other participants were asked to calculate:

- total concentration of iodine in the aqueous phase ($mol \cdot dm^{-3}$);
- total concentration of iodine in the gas phase ($mol \cdot dm^{-3}$);
- speciation of iodine in the aqueous phase (I_2, HOI, I^-, IO_3^-, I_2OH^-, etc.);
- speciation of iodine in the gas phase (I_2, HOI);

as a function of time in 1 h intervals; and

- distribution of iodine at the end of the test (mass in aqueous and gas phases and on surfaces exposed to the gas and aqueous phases).

Those participants who had a water radiolysis model were also asked to calculate:

- H_2O_2 and H_2 concentrations as a function of time in 1 h intervals.

This report presents a detailed description of the RTF tests used for the exercise, a brief description of the models/codes used and the modelling process and the description and interpretation of the results.

2. DESCRIPTION OF THE RTF TESTS

Intermediate-scale studies on which the ISP-41 was based, were performed in the Radioiodine Test Facility (RTF) at AECL's Whiteshell laboratories. A diagram of the RTF is shown in Figure 1. A brief description of the facility and of the test is presented here.

2.1 Radioiodine test facility

The RTF consists of a replaceable, cylindrical main vessel into which a ^{60}Co radiation source can be placed. In 1992, when the data for this exercise was collected, the radiation source provided an absorbed radiation dose rate of about 1.4 $kGy \cdot h^{-1}$ in the aqueous phase. (The absorbed dose rate decreases with time as the cobalt source decays with a half-life of 5.3 years.) The main vessel can be partially filled with water and selected chemical additives can be added to the aqueous phase to simulate the sump water in containment following an accident. Typically, the aqueous and gas volumes are 25 and 315 dm^3, respectively; the surface areas in contact with the aqueous and gas phases are 52 and 220 dm^2, respectively; and the aqueous and gas-phase interfacial area is 37 dm^2. Electrical heaters around the outside of the vessel can control the temperature of the vessel walls in contact with the gas phase up to 110°C and the water temperature up to 90°C. A test is generally initiated with an injection of ^{131}I labelled CsI into the aqueous phase, to provide an initial aqueous iodide concentration of about 1×10^{-5} $mol \cdot dm^{-3}$. This is followed by on-line and off-line monitoring of various species, listed in Table 1. At the end of a test, the iodine surface loadings are determined by washing the vessel by measuring the ^{131}I activity in the washes and the remaining activity on the surfaces. The final iodine activities on the coupons placed both in the gas and the aqueous phases during the tests are also used to determine and confirm the iodine surface loadings.

Table 1. **RTF Data**

Aqueous Phase - Online	**Gas Phase - Online**
Total Iodine Oxidation Reduction Potential Dissolved Oxygen pH	Total Iodine Hydrogen
Aqueous Phase - Off-line	**Gas Phase - Off-line**
Total Iodine Concentration Iodine Speciation Anions Metal Ions Organic Compounds (HPLC) Hydrogen Peroxide	Total Iodine Iodine Speciation Gas Composition (Mass Spectrometry) Organic Compounds (GC)

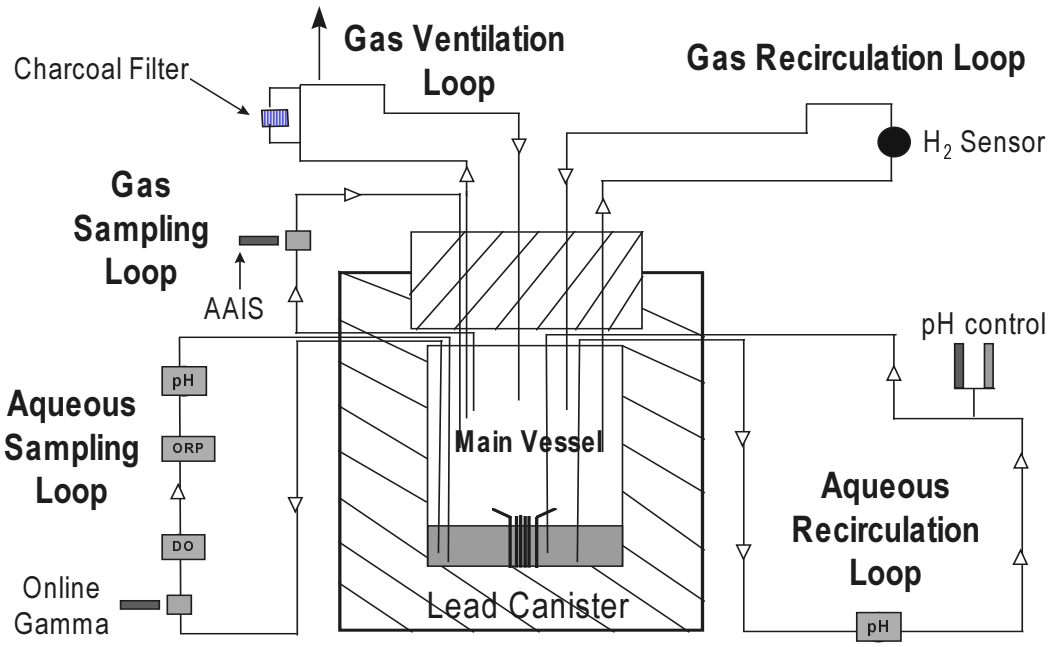

Figure 1: **Schematic diagram of the radioiodine test facility**.

2.2 Experimental

Conditions:

Operating conditions for Stage 1 and Stage 2 of the ISP experiment are presented in Table 2.

Table 2. **Experimental Conditions For ISP-41 RTF Experiments**

Vessel	316 Stainless Steel
Dose Rate	~ 1.36 $kGy \cdot h^{-1}$
Temperature	25°C (± 3 °C)
Starting Conc.*	9×10^{-6} $mol \cdot dm^{-3}$ CsI (± 10%)
Aqueous Volume	25 dm^3 (± 10%)
Gas Volume	315 dm^3 (± 1%)
Starting pH	~ 10 (± 0.3)
Aqueous Surface Area	52 dm^2
Interfacial Surface Area	37 dm^2
Gas Surface Area	220 dm^2

* Note: Speciation of the ^{131}I tracer prior to test start indicated 99.88% of the solution was in the form of I^- with 0.11 percent in the form of IO_3^- and 0.01% in the form of organic iodide.

Sequence of events

The ^{60}Co source was loaded into the RTF main vessel several days before the initiation of Stage 1 of the test. Two days prior to beginning the test, the vessel was filled with distilled water. Shortly before the addition of the ^{131}I labelled CsI solution solution (2 h) the vessel was drained, rinsed several times with distilled water, until chromatographic analysis showed that the gas and aqueous phases were free of organic contaminants, and refilled with a fresh charge of 25 dm^3 of distilled water which was then adjusted to pH 10 by additions of LiOH. The vessel was then purged with CO_2 free air. Speciation analysis of the tracer labelled CsI solution was done prior to adding it to the main vessel, and estimated it to contain 99.88 % I^-, 0.11 % IO_3^-, and 0.01 % organic iodide and I_2. The CsI solution was then added to the vessel via the aqueous sampling loop to provide a concentration of 9×10^{-5} $mol \cdot dm^{-3}$ in the aqueous phase. A sequence of events for Stage 1 is presented in Table 3.

Table 3. **Experimental events - Stage 1**

Time (h)	Event
0	Tracer Added - pH 10
23.6	pH control set to 9
96.5	pH control set to 8.5
164.7	Unscheduled pH excursion to 7.8
166.7	pH control set to 8.5
181.7	Unscheduled pH excursion to 7.8
190.7	pH control set to 8.5
195.5	pH control set to 8.2
264	pH control set to 7.9
312	pH control set to 7.6
339	pH control set to 7.4
363.4	Charge Dumped - Vessel Washed

At 363 h, the charge in the vessel was drained, and water adjusted to pH 10 was added from the top of the vessel via a spray-header. Since this process would wash the walls of the vessel and remove soluble iodine species from the surfaces, data obtained after this time is not considered as part of the test exercise.

Between Stage 1 and Stage 2, the vessel was washed repeatedly until the water was free of iodine as determined by γ-counting of samples of the wash water. The gas phase of the vessel was also continuously purged with air during this period and recirculation was continued through the loops to remove adsorbed iodine. On-line detection of the gas phase was also continued during this period. When γ-counting of the gas phase indicated that the iodine concentrations were below detection limits, the vessel was refilled with a fresh charge of distilled water, which was set to pH 10. ^{131}I-labelled CsI solution (the same tracer solution as used in Stage 1) was again added via the aqueous sampling loop. The sequence of events for stage 2 is tabulated in Table 4.

Table 4 **Experimental events - Stage 2**

Time (h)	Event
0	Tracer Added - pH 10
23	pH control set to 8.5
45	pH control set to 7.9
118	pH control set to 6.5
168	pH control set to 5.5
192	pH control set to 10
285	Charge dumped, Vessel Washed

Mass balance

Estimates of the mass balance provided in Section 4 were obtained simply by assuming that all of the iodine unaccounted for in the aqueous and gas phases was retained on the vessel gas phase surfaces. Although this is rather simplistic, stainless steel coupons retrieved from the aqueous phase of the vessel indicated that negligible amounts of iodine were retained on these surfaces, whereas γ-counting of the vessel, vessel loops and gas recirculation pump diaphragm indicated extensive adsorption occurred on these surfaces. Unfortunately accurate estimates of the quantity of iodine on these surfaces could not be obtained because not all of them were accessible (e.g. inside the loops) or of a suitable geometry (vessel walls) to obtain reliable counting data. Furthermore, adsorption of iodine on the gas phase surfaces was highly localised.

2.3 Test results

Observed gas phase and aqueous phase iodine concentrations for Stage 1 and Stage 2 are presented in Figures 2 and 3.

a)

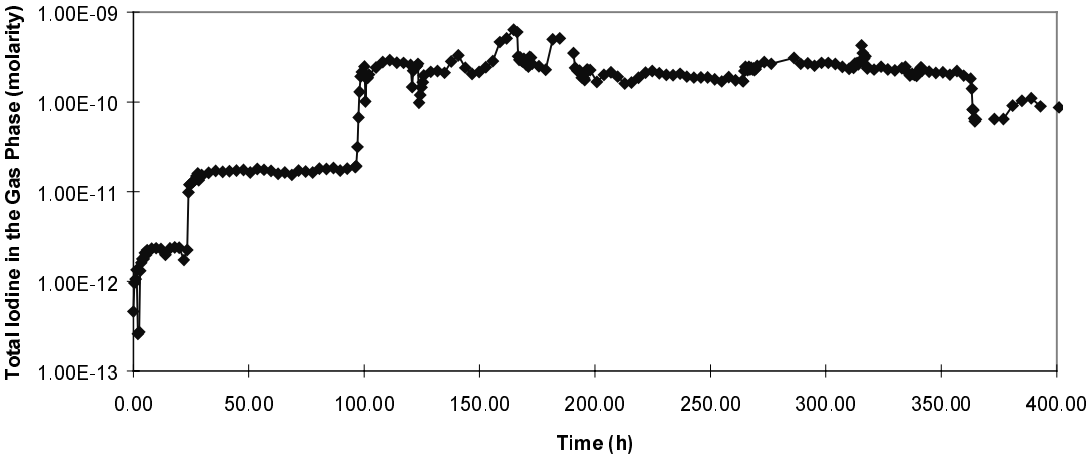

b)

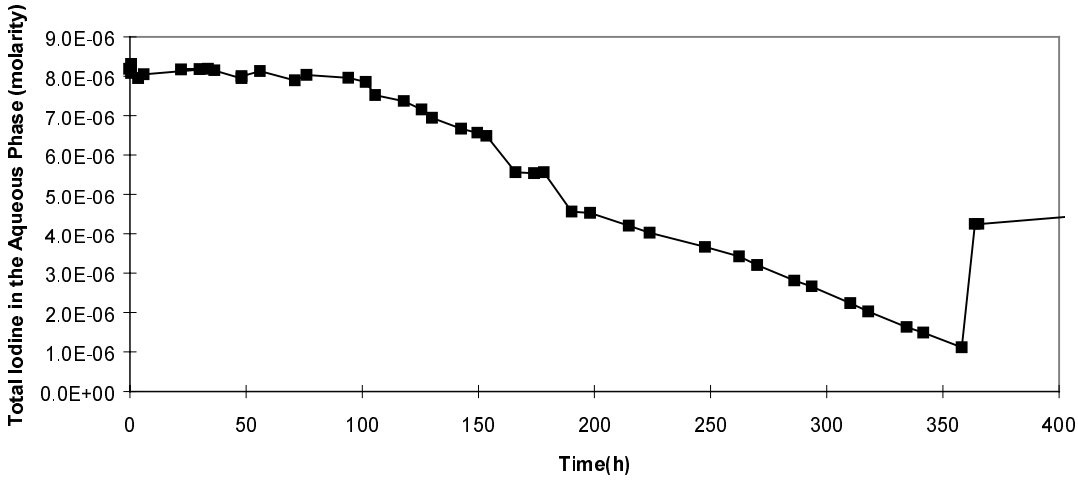

Figure 2. **Measured total concentrations of iodine in Stage 1: (a) Gas Phase and (b) Aqueous Phase**.

(a)

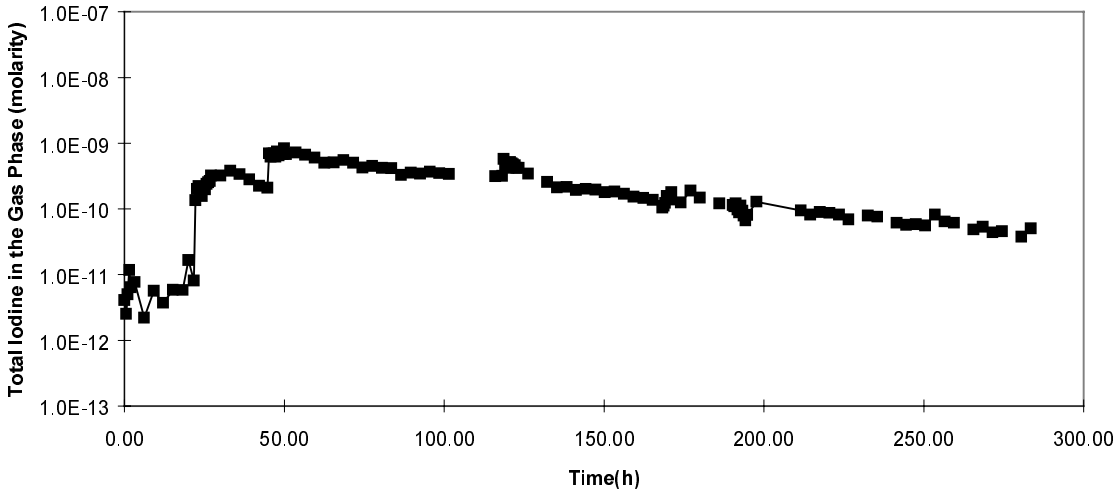

(b)

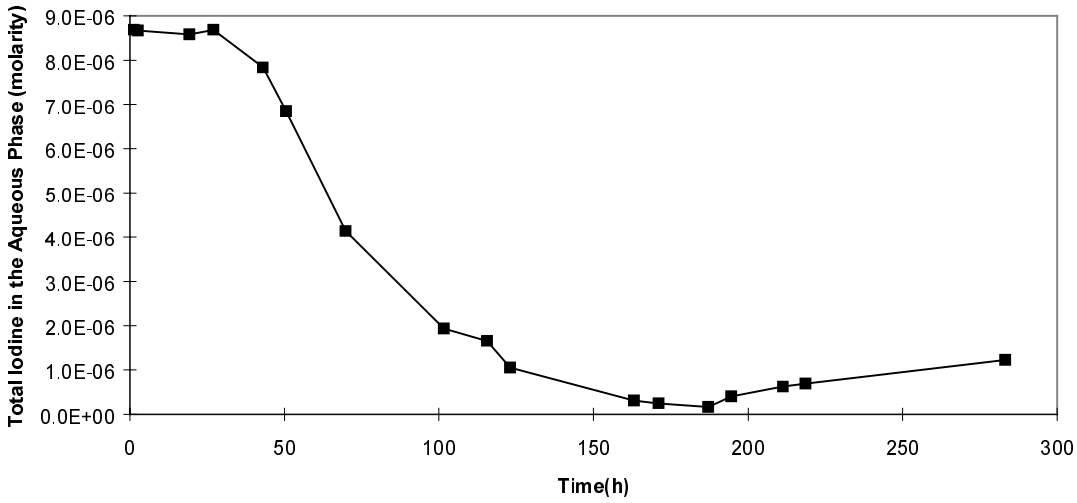

Figure 3. **Measured total concentrations of iodine in Stage 2: (a) Gas Phase, and (b) Aqueous Phase**.

3. DESCRIPTION OF THE CODES

The codes used by the participants were LIRIC (AECL), MELCOR-I (Sandia), IMPAIR (PSI, Siemens, GRS, and JAERI) and IODE (CIEMAT, IPSN and NRIR). Detailed descriptions of these codes are given in Appendix A and Reference 1. A brief description of the codes is provided here for the purposes of comparing the calculations performed for the ISP-41 exercise.

3.1 Gas-aqueous interfacial mass transfer and adsorption

All of the codes used in the ISP-41 comparison treat mass transport and surface adsorption in a similar manner. Mass transport across the gas-aqueous interface is modelled in all cases using the model for diffusion through a stagnant film:

$$\frac{dC_{aq}}{dt} = k_t \cdot \frac{A_{aq}}{V_{aq}} \cdot (H \cdot C_g - C_{aq}) \quad (1)$$

$$\frac{dC_g}{dt} = k_t \cdot \frac{A_{aq}}{V_g} \cdot (C_{aq} - H \cdot C_g) \quad (2)$$

where C_{aq} and C_g are the aqueous- and gas-phase concentration of a given species, k_t is the overall (or gas-aqueous phase interfacial) mass-transfer coefficient (i.e., $1/k_t = 1/k_{aq} + H/k_g$), A_{aq} is the gas/aqueous phase interfacial area, V_{aq} is the aqueous-phase volume, V_g is the gas-phase volume, and H is the partition coefficient.

Surface adsorption in all of the codes is treated as a reversible adsorption-desorption process. For example, the formulation in LIRIC for adsorption on gas phase surfaces is:

$$\frac{d[I_2]_g}{dt} = -\nu_{Ad} \cdot \frac{A_{gs}}{V_g} \cdot [I_2]_g \cdot \left(1 - \frac{[I_2]_s}{[I_2]_s^o}\right) + k_{Des} \cdot \frac{A_{gs}}{V_g} \cdot [I_2]_s \quad (3)$$

where $[I_2]_g$ and $[I_2]_s$ are the molecular iodine concentrations in the gas phase ($mol \cdot dm^{-3}$) and on the surface ($mol \cdot dm^{-2}$), respectively, ν_{Ad} is the deposition velocity ($dm \cdot s^{-1}$), k_{Des} is the desorption rate constant (s^{-1}), A_{gs} and V_g are the gas-phase surface area (dm^2) and volume (dm^3), respectively, and $[I_2]_s^o$ is the saturation capacity of the surface for I_2 ($mol \cdot dm^{-2}$). Although the code has a built in method for accommodating a case where the surface becomes saturated, the saturation capacity $[I_2]_s^o$ has, for this exercise, been set high enough that the adsorption rate is not influenced by it. The same type of expression is used for aqueous phase surface adsorption. IODE, IMPAIR and MELCOR-I have similar formulations for adsorption.

3.2 Aqueous phase iodine chemistry

Thermal iodine reactions

IMPAIR, IODE, LIRIC and MELCOR-I model hydrolysis of iodine in much the same manner, with the overall reactions being:

$$I_2 + H_2O = HOI + I^- + H^+ \quad (4)$$

$$HOI = OI^- + H^+ \quad (5)$$

$$3HOI = IO_3^- + 2I^- + 3H^+, \quad (6)$$

where Reactions (4) and (5) are in rapid equilibrium. Although the reaction rate formulation of Reaction (6) does differ between the codes, calculations performed with IODE and IMPAIR have shown that the difference in modelling approaches has little impact on iodine volatility. Sensitivity studies performed with

LIRIC also show that Reaction (6) is unimportant under radiolytic conditions. Both LIRIC and MELCOR-I contain a more detailed breakdown of Reaction (4), which involves the formation of I_2OH^-. This species participates in the reduction of I_2 by H_2O_2 , and is therefore necessary for inclusion in the mechanistic codes. In IODE and IMPAIR, reduction of molecular iodine is captured by an empirical formulation however, thus the I_2OH^- equilibria are excluded in these codes.

Radiolytic reactions of iodine species

It is only in the radiolytic reaction set that the mechanistic and empirical codes diverge to a great extent. In LIRIC and MELCOR-I, a mechanistic model is used for calculating the concentrations of the water radiolysis species e^-, H^+, H_2, •H, H_2O_2 and •OH, which subsequently react with various iodine and organic species to produce volatile iodine species. Neglecting the radiolysis of organic species and the formation of organic iodides, LIRIC still contains about 300 reactions. The key ones are:

$$4.1\ H_2O \xrightarrow{h\nu} 2.6\ e_{aq}^- + 0.6\ \bullet H + 2.7\ \bullet OH + 0.7\ H_2O_2 + 2.6\ H^+ + 0.45\ H_2 \qquad (7)$$

$$I^- + \bullet OH \rightarrow I\bullet + OH^- \qquad (8)\ [1]$$

$$I\bullet + I\bullet \rightarrow I_2 \qquad (9)\ [1]$$

$$I_2(aq) + H_2O \rightarrow HOI + I^- + H^+ \qquad (10)\ [1]$$

$$I_2(aq) + 2O_2^- \rightarrow 2I^- + O_2 \qquad (11)\ [1]$$

$$I_2(aq) + H_2O_2 \rightarrow 2I^- + 2H^+ + O_2 \qquad (12)\ [1]$$

The empirical codes IODE and IMPAIR essentially use two equations to model radiolysis of iodine species in the aqueous phase. In IODE, the equations are:

$$2\ I^- \xleftrightarrow{h\nu} I_2 \qquad (13)$$

$$2\ IO_3^- \xleftrightarrow{h\nu} I_2 + 3\ O_2 \qquad (14)$$

The pH dependence of molecular iodine formation in IODE is accommodated by incorporating $[H^+]$ into the rate equation in the following manner:

$$\text{Rate of } I_2 \text{ production by (13)} = -d[I_2]/dt = -k_{13}[I^-]\cdot[H^+]^n\cdot D + k_{-13}[I_2]\ , \qquad (15)$$

$$\text{Rate of } I_2 \text{ production by (14)} = -d[I_2]/dt = -k_{14}[IO_3^-]\cdot[H^+]^n\cdot D + k_{-14}[I_2] \qquad (16)$$

where D is the dose-rate in $Gy\cdot s^{-1}$, and the default values for the rate constants are:

$k_{13} = k_{14} = 2.5 \times 10^{-4}\ (mol\cdot dm^{-1})^{-0.25}\ Gy^{-1}$
$k_{-13} = k_{-14} = 2 \times 10^{-5}\ s^{-1}$
$n = 0.25$

1. Represents many reaction steps (i.e., more than one reaction is involved).

For IMPAIR, Reaction (13) is the same as that for IODE, with D expressed in $kGy \bullet h^{-1}$ however instead of Reaction (14), iodate is irreversibly converted to iodide rather than to molecular iodine:

$$IO_3^- \xrightarrow{h\nu} I^- \qquad (17)$$

with the rate of Reaction (17) expressed as:

$-d[IO_3^-]/dt$ of $k_{17}[IO_3^-]^{-1.3} \cdot D$.

where D is the dose-rate in $kGy \bullet h^{-1}$. Default values for k_{13}, k_{-13} and k_{17} for IMPAIR are:

$k_{13} = 4.0 \times 10^{-6}$ $(mol \bullet dm^{-1})^{-0.1}$ kGy^{-1}
$k_{-13} = 2 \times 10^{-7}$ s^{-1}
$k_{17} = 0.01$ s^{-1}
n = 0.1

3.3 Effect of organic species

The formation and decomposition of organic iodide and radiolysis of organic species are also treated quite differently in LIRIC than in IODE and IMPAIR. In the former, the effect of aqueous organic species on pH, dissolved oxygen concentration and organic iodide formation are modelled by a series of reactions, which have been developed from detailed mechanistic studies of methyl ethyl ketone. Organic iodide formation is assumed to be primarily an aqueous phase process. Decomposition of organic iodides by hydrolysis is also incorporated into the model.

$$RH + \bullet OH \rightarrow R\bullet + H_2O \qquad (18)$$
$$R\bullet + O_2 \rightarrow RO_2\bullet \rightarrow \bullet R', \text{ alcohols, aldehydes, acids and } CO_2 \qquad (19)$$
$$R\bullet + I_2 \rightarrow RI + I\bullet \qquad (20)$$

In IODE and IMPAIR organic iodide formation is modelled by using (CH_3I) as a generic organic iodide. It can be formed both by surface processes in the aqueous phase, or by homogeneous gas phase processes such as:

$$I_2 + 2\,CH_3R\bullet \rightarrow 2\,CH_3I + 2R\bullet \qquad (21)$$
$$CH_3I \xleftrightarrow{h\nu} 2\,CH_3\bullet + I_2 \qquad (22)$$

IMPAIR uses HOI as the reacting species as well, and in some versions, can differentiate between high molecular weight organic iodides (formed from $CH_3R\bullet$) and methyl iodide. In IMPAIR, organic iodide formation on painted surfaces depends only on the deposited I_2 and I^- (sump) concentrations. The concentrations of $CH_3R\bullet$, and $CH_3\bullet$ are not quantified, but are assumed to be in large excess. Homogeneous formation of organic iodide is modelled only for the sump, and the concentrations of the reacting species $CH_3R\bullet$ and $CH_3\bullet$ are provided by the user. Formation rate constants were derived from ACE/RTF Test 2A and 3B data.

In the experiment on which ISP-41 exercise was based, there was no significant source of organic impurities to promote organic iodide formation in either phase other than impurities in the ^{131}I tracer used to label the initial CsI solution, and perhaps some small amounts of organic impurities on the vessel or loop

surfaces and in the atmosphere. Consequently, most of the participants chose to ignore organic iodide formation in the both sets of calculations, and those who did incorporate a nominal amount of organic or organic iodide as part of the initial conditions found that organic iodides did not contribute significantly to the calculated total gas phase iodine concentration (see Figure 19 Appendix B).

3.4 Gas phase reactions

Although both IMPAIR and IODE contain equations for formation of iodine oxides by reaction of iodine with ozone, and gas phase surface reactions for formation of organic iodides, none of the participants used these reactions in their simulations, therefore it is difficult to judge how important these reactions are in determining iodine volatility. Gas phase reactions, aside from surface adsorption are not incorporated into LIRIC, because in comparison to homogeneous aqueous phase reactions, homogeneous gas phase reactions are considered to be unimportant.

4. RESULTS

The first set of calculations done by the participants, and the rate constants used to obtain these results are presented in Appendix B. In general, all the codes calculated gas phase iodine concentrations reasonably well, however the aqueous phase iodine concentrations were overestimated, and the amount of iodine on surfaces was underestimated significantly. Despite this, analysis of the first set of calculations indicated that the key phenomena influencing iodine behaviour, ranked in order of the most important to least important were:

1) radiolysis (pool chemistry);

2) adsorption/desorption behaviour;

3) mass transfer.

In the first set of calculations, use of different adsorption/desorption rate constants and mass transfer coefficients by each of the participants made it difficult to compare the pool chemistry model in each code. The adsorption desorption and mass transfer models within the various codes are very similar. Adsorption/desorption and mass transfer behaviour are also very dependent upon experimental (or accident) specific conditions, and the input rate constants used for these phenomena must necessarily reflect the conditions for which the code is being used. It is only the radiolysis models, and the rate constants for these models, which can be compared in a systematic manner to determine the adequacy of the various iodine behaviour codes. It was therefore decided, at a meeting held in Ottawa in October 1998, that each participant should repeat the calculations using a standard set of rate constants for adsorption and mass transfer (these rate constants were recommended for the RTF test conditions by AECL and are discussed in Section 5.1).

For the rate constants for radiolysis in the aqueous phase, it was recommended that each participant should initially use code default values, or the same set of values used for the first calculation. Participants were also encouraged to submit calculations performed after optimising their radiolysis models by changing these values. Repeating the calculations also addressed other concerns that:

1) Prior knowledge of the test results (and of the appropriate adsorption/desorption rate constants to use) was a factor in code performance.

2) Evaluation of overall code performance would be unduly biased by the choice of adsorption/desorption rate constants. Most of the values used by the participants were obtained from experiments performed at higher temperatures more applicable to anticipated post accident containment conditions, and therefore underestimated the effect of adsorption on iodine behaviour at room temperature.

The total gas phase and aqueous phase iodine concentrations calculated in the second set of the exercise, along with experimentally determined values are shown in Figures 1-18 in Appendix C. Important features and discrepancies between the calculations are discussed below.

4.1 Total concentration of iodine in the gas and aqueous phases

Although most of the initial calculations predicted the gas phase iodine concentrations observed in the RTF test to within an order of magnitude (see Figures 1-18 in Appendix B), results from the second set of calculations are significantly worse. For example, many of the calculations underestimated iodine volatility by over an order of magnitude at pH values greater than 6 (See Figures 1-18 in Appendix C).

Table 5. **Calculated Vs. experimental iodine distribution at test end 1st calculation**

	Stage 1 Percentage Iodine Inventory at Test End[a]				**Stage 2 Percentage Iodine Inventory at Test End**			
	Gas	Aq.	Gas walls	Aq. walls	Gas	Aq.	Gas walls	Aq. walls
CIEMAT[b] (Case 1)	.006	93.3	6.7	-	.006	85.9	14	-
CIEMAT[b] (Case 2)	.004	91.7	5.0	3.32	.005	81.4	10.1	
CIEMAT[b] (Case 3)	.03	55.7	44	-	.012	43.7	56.3	-
CIEMAT[b] (Case 4)	.019	44.4	33.2	22.2	.008	32.8	36	30.9
IPSN	.03	91	8.7	-	.02	88	12	-
NRIR	.04	10	89	-	.01	20.6	79	-
Siemens	.6	99.4	1.5×10^{-5}	-	2.6×10^{-4}	100	1.1×10^{-4}	-
GRS	.34	99.7	3.5×10^{-4}	-	2.6×10^{-4}		1.8×10^{-4}	-
PSI	.4	99.6	3.5×10^{-6}	-	3.5	96.4	9.5×10^{-5}	-
JAERI	.14	40.6	59.3	-	.08	88.3	11.7	-
Sandia	.007	24	76	-	.002	25.5	74.5	-
AECL	0.03	10.8	89.7		.003	16.4	83.6	
Experiment	**.02**	**12.4**	**87.6**	-	**.007**	**13.6**	**86.4**	-

[a] Test end defined to be at 363 h, when the contents of the sump were drained.

[b] Case 1: $k_{13} = 1.7 \times 10^{-3}$ Gy^{-1}, $k_{-13} = 2 \times 10^{-5}$ s^{-1}, n=0.5 no aqueous phase adsorption
Case 2: $k_{13} = 1.7 \times 10^{-3}$ Gy^{-1}, $k_{-13} = 2 \times 10^{-5}$ s^{-1}, n=0.5 aqueous phase adsorption
Case 3: $k_{13} = 2.5 \times 10^{-4}$ Gy^{-1}, $k_{-13} = 2 \times 10^{-5}$ s^{-1}, n=0.25 no aqueous phase adsorption
Case 4: $k_{13} = 2.5 \times 10^{-4}$ Gy^{-1}, $k_{-13} = 2 \times 10^{-5}$ s^{-1}, n=0.25 aqueous phase adsorption

Table 6. **Calculated Vs. experimental iodine distribution at test end: 2nd calculation**

	Stage 1 Percentage Iodine Inventory at Test End[a]			**Stage 2 Percentage Iodine Inventory at Test End**		
	Gas	Aq.	Gas walls	Gas	Aq.	Gas walls
CIEMAT[b] (Case 1)	1.1×10^{-4}	87.8	12.2	2.3×10^{-4}	75.4	24.6
CIEMAT[b] (Case 2)	4.9×10^{-4}	20.6	79.4	4.3×10^{-4}	30.2	69.8
CIEMAT[b] (Case 3)	4.9×10^{-4}	1.1	98.9	7.5×10^{-4}	22.9	77.1
CIEMAT[b] (Case 4)	4.9×10^{-4}	13.7	86.3	5.1×10^{-4}	34.7	65.3
CIEMAT[b] (Case 5)	1.8×10^{-4}	76.6	23.4	2.8×10^{-4}	85	15
IPSN	2.1×10^{-4}	88.9	11.1	0.002	93.5	6.5
NRIR	0.017	6.7	93.3	0.007	13	87
Siemens	8.6×10^{-3}	70	30	0.010	51.1	48.9
GRS	1.6×10^{-3}	76	24	3.1×10^{-3}	50.7	49.3
PSI	2.0×10^{-6}	100	0	2.9×10^{-6}	100	0
JAERI	0.020	41.6	58.4	0.016	60.4	39.6
Sandia	.007	24	76	.002	25.5	74.5
AECL	0.024	10.0	89.9	.004	12.5	87.5
Experiment	**.02**	**12.4**	**87.6**	**.007**	**13.6**	**86.4**

[a] Test end defined to be at 363 h, when the contents of the sump were drained.
[b] Case 1: $k_{13} = 1.7\times10^{-3}$ Gy^{-1}, $k_{-13} = 2\times10^{-5}$ s^{-1}, n=0.5 no aqueous phase adsorption
Case 2: $k_{13} = 2.5\times10^{-4}$ Gy^{-1}, $k_{-13} = 2\times10^{-5}$ s^{-1}, n=0.25 no aqueous phase adsorption
Case 3: $k_{13} = 2.17\times10^{-4}$ Gy^{-1}, $k_{-13} = 2\times10^{-5}$ s^{-1}, n=0.1 no aqueous phase adsorption
Case 4: $k_{13} = 2.17\times10^{-5}$ Gy^{-1}, $k_{-13} = 2\times10^{-5}$ s^{-1}, n=0.1 no aqueous phase adsorption
Case 5: $k_{13} = 2.17\times10^{-5}$ Gy^{-1}, $k_{-13} = 2\times10^{-5}$ s^{-1}, n=0.1 no aqueous phase adsorption

The agreement between the observed and calculated aqueous phase iodine concentrations was slightly better for the second set of calculations (Table 6) than for the first (Table 5), however 5 out of 8 of the calculations significantly overestimated (by more than 30%) the final aqueous phase concentrations. These cases likewise considerably underestimated the amount of iodine adsorbed on surfaces (also listed in Table 6).

4.2 Speciation and distribution of iodine

Since there were no significant sources of organic impurities in the experiments modelled by this exercise, organic iodide formation was not explicitly treated by many of the participants. In most calculations, organic iodides were found to contribute very little to the fraction of volatile iodine species in the gas phase. An organic iodide impurity in the ^{131}I tracer of 0.01% (equivalent to 10^{-9} mol•dm^{-3}) was provided as input into some of the calculations, and JAERI calculations also assumed that a high molecular weight organic iodide was present as an impurity in the aqueous phase. This led to a significant fraction of iodine at high pH being in the form of high molecular weight organic iodides in their calculations (See Figures 13 and 14 Appendix B and C). In the aqueous phase, all the calculations predict that iodide was the

predominant species. The fraction of aqueous iodine predicted to be in the form of iodate differs fairly dramatically between the codes however in most cases less than 10% of the original iodine inventory is calculated to be in the form of iodate at the end of the test. Experimental results show that a maximum of 1 % of the original iodide inventory was converted to iodate (See Figure 20 Appendix B.)

5. DISCUSSION

In assessing whether of not the calculations performed were a good fit to the data, two overall criteria were used[2]. These were:

1) Did the calculations reproduce the observed gas phase iodine concentrations to within an order of magnitude for all pH values?

2) Did the code reproduce (within 20%) the aqueous phase iodine concentration as a function of time?

A more rigorous criterion was chosen for the aqueous phase iodine concentration because:

1) its time dependent behaviour gives a clearer representation of what is happening to the iodine inventory (i.e. conversion to volatile iodine followed by depletion to the gas phase surfaces) than does the gas phase iodine concentration; and

2) the aqueous phase iodine concentration is the more critical parameter controlling overall iodine behaviour. As a prerequisite to applying iodine behaviour codes to complex systems, it is important that it be demonstrated that the iodine codes could adequately represent the aqueous phase iodine concentrations for the rather simple experiments on which this ISP was based.

Based on these criteria, only three out of nine of the first set of calculations, and four out of nine of the second set could be considered to be a success. The large differences observed between the various calculations, even those performed using the same code, demonstrate that in most cases, the codes are extremely sensitive to rate constants which are user defined. These sensitivities are discussed in the following sections.

5.1 The effect of adsorption/desorption and interfacial mass transfer

One of the most significant differences between the various calculations is the amount of iodine that is predicted to deposit on surfaces (Tables 5 and 6). To some extent, the amount of iodine lost from the aqueous phase to gas (or aqueous) surfaces can be adjusted in each code by variation in the adsorption-desorption rate constants. This is nicely demonstrated in the first set of calculations performed by CIEMAT, in which the sensitivity of the code to adsorption/desorption rates in the aqueous phase was examined (see Figures 1 and 2, Appendix B). LIRIC uses adsorption-desorption rate constants that were derived from both intermediate-scale and bench-scale studies and have been used to successfully model several RTF experiments. It is therefore not surprising that for the first set of calculations done by the participants, those which provided the best fits to the data were those which used adsorption-desorption rate constants similar to those used in LIRIC. However, although the use of the “correct” adsorption/desorption rate constants was one of the criteria for obtaining a reasonable fit to the data, it was

2. These criteria are for the purpose of this ISP exercise only.

not in itself sufficient to reproduce the experimental results. This became evident in the second set of calculations, in which everyone used the same adsorption/desorption rate constants (9×10^{-3} dm•s^{-1} and 9×10^{-7} s^{-1} for adsorption and desorption respectively). Most of the calculations still greatly underestimated the amount of iodine adsorbed on surfaces because the radiolysis models underestimate the I_2 production rate in the aqueous phase (See Section 5.2).

The interfacial mass transfer coefficient also plays a role in determining the gaseous iodine fraction, and the rate at which iodine is adsorbed on the gas phase surfaces. Measurements of interfacial mass transfer rates in the RTF experiments which have similar flow rates as this experiment provided an approximate interfacial mass transfer coefficient on the order of 10^{-4} dm·s^{-1}. Sensitivity studies, performed with LIRIC on a variety of RTF experiments under similar conditions, have shown that use of a value for the overall mass transfer coefficient (k_t) for I_2 which is lower than about 2×10^{-4} dm·s^{-1} results in mass transfer from the aqueous to the gas phase becoming the rate determining step for accumulation of iodine in the gas phase. Therefore, in the interests of providing conservative estimate for iodine volatility, LIRIC uses mass transfer coefficients for I_2 which are high enough so that mass transfer is not rate limiting (around 5×10^{-4} dm·s^{-1} at 25ºC). This value approaches the limiting value for transfer across an aqueous/gas interface from a pool [2].[3] In order to provide a better comparison between the pool chemistry component of each of the codes, it was recommended for the second set of calculations, that this be the value used by all the participants since some of the participants used overall mass transfer coefficients which were considerably different than this value for their first set of calculations.

Although mass transfer and surface adsorption do have some effect on iodine volatility, and the amount of iodine distributed between the gas phase, aqueous phase and surfaces, it is the pool chemistry component of the codes which truly controls the codes ability to predict iodine behaviour. Use of the appropriate rate constants to describe the transport of volatile iodine species from one place to another is important, but accurate modelling of iodine behaviour requires knowing how much of that species is available to be transported. The second set of calculations showed that, even using the same mass transfer and adsorption/desorption rate constants, the adsorption of iodine on surfaces was greatly underestimated in many cases. This is because the rate of conversion of iodide to molecular iodine in the aqueous phase was underestimated by many of the codes. (See Section 5.2)

A final note regarding the choice of rate constants for adsorption/desorption and mass transfer is that there are some physical limitations as to what these rate constants can be. The adsorption rate constant for example, can never exceed the gas phase mass transfer coefficient, since in the limiting case, adsorption on a surface can only be as fast as the species can reach the surface. A similar limit exists for the interfacial mass transfer coefficient whose value is limited by the rate constants for gas or aqueous phase mass transfer. In the first set of calculations performed by Sandia, a mass transfer coefficient of 1.2×10^{-3} dm·s^{-1} was used. This value is considered to be a bounding value for mass transfer from a vigorously mixed system, in which there is no resistance to transfer in the aqueous phase.[3] It is extremely unlikely that the flow conditions in the RTF could result in values this high.

3. An upper limit of about 0.1 dm•s^{-1} has been observed for the gas phase mass transfer coefficient k_g in vigorously mixed systems [1]. The maximum value for the interfacial mass transfer coefficient k_t, defined by $1/k_t = 1/k_a + H/k_g$ (H, the partition coefficient of I_2 is about 80 at 25 °C) would be 1.2×10^{-3} dm·s^{-1} if there was no liquid phase resistance to transfer ($1/k_a = 0$). In general however k_a is an order of magnitude less than k_g.

5.2 The radiolysis model

The second set of calculations demonstrated that even when everyone used the same adsorption/desorption rates and mass transfer coefficients, there was a large difference between the various codes (even different versions of the same code) in the predicted gas and aqueous phase iodine concentration. This confirmed that the model for radiolysis of iodine in the aqueous phase is the key to the ability of any code to predict both the volatility and distribution of iodine. The iodine radiolysis model or pool chemistry model is also the area in which there appears to be the largest variation both in modelling approach (semi-empirical vs. mechanistic) and in user defined kinetic rate constants.

A Comparison between the semi-empirical codes, IODE and IMPAIR

A compilation of the rate constants used as input for IODE and IMPAIR codes for the second set of calculations are tabulated in Table 7 and a demonstration of the sensitivity of the code IODE to the choice of rate constants for radiolytic oxidation of iodide is presented in the calculation results performed by CIEMAT (Figure 4). It is not surprising that the range of radiolytic rate constants presented in Tables 7 resulted in a wide range of values for the concentrations and distribution of iodine being predicted by each code for this ISP experiment.

The range of values for radiolytic rate constants presented in Table 7 demonstrates that the IMPAIR and IODE codes are still in the evolutionary stage where rate constants are being changed and optimised by the users to provide a best fit to data as that data becomes available. Adjustment of the rate constants so that a code adequately reproduces results from one experiment does not necessarily mean that the code can be used to reproduce other experiments. JAERI found that although they had adjusted the rate constants in IMPAIR to simulate results from ACE 3B, they could not reproduce the RTF experiments performed at AECL in a vinyl painted vessel with the same rate constants (see Appendix A). As another example, IODE version 4.1 rate constants were used in this exercises by IPSN and in one of the cases presented by CIEMAT, however version 4.2, which has been used to model the PHEBUS RTF experiments uses rate constants which are considerably different [3]. Whether version 4.2 of IODE can be applied successfully to model experiments from which earlier versions of IODE were derived is unclear.

Table 7. **Radiolysis rate constants used in iode and impair: 2nd calculation**

	k_{13} $(mol \cdot dm^{-3})^{-n}$	$k_{-13}(s^{-1})$	n_1	$k_{13} \cdot D \cdot [H^+]^n$ at pH 5 (s^{-1})	$k_{17}(s^{-1})^{-0.3}$	n_{17}
IMPAIR PSI	3×10^{-5} kGy^{-1}	2×10^{-7}	0.35	3.6×10^{-5}	5×10^{-5}	1.3
IMPAIR Siemens	2.3×10^{-4} kGy^{-1}	2×10^{-7}	0.1	4.5×10^{-3}	5×10^{-5}	1.3
IMPAIR GRS	2.3×10^{-4} kGy^{-1}	2×10^{-7}	0.4	1.5×10^{-5}	5×10^{-5}	1.3
IMPAIR JAERI[a]	4.0×10^{-6} kGy^{-1}	1×10^{-15}	0.1	7.9×10^{-5}	5×10^{-5}	1.3
IODE CIEMAT[b,c]	1.7×10^{-3} Gy^{-1}	2×10^{-5}	0.5	2.1×10^{-6}	n.a.	n.a.
IODE CIEMAT[b,c]	2.5×10^{-4} Gy^{-1}	2×10^{-5}	0.25	5.5×10^{-6}	n.a.	n.a.
IODE CIEMAT[b,c]	2.17×10^{-4} Gy^{-1}	2×10^{-5}	0.1	2.7×10^{-5}	n.a.	n.a.
IODE CIEMAT[b,c]	2.17×10^{-5} Gy^{-1}	2×10^{-5}	0.1	2.7×10^{-6}	n.a.	n.a.
IODE CIEMAT[b,c]	2.17×10^{-6} Gy^{-1}	2×10^{-5}	0.1	2.7×10^{-7}	n.a.	n.a.
IODE NRIR[b]	0.1 Gy^{-1}	0	0.5	3.2×10^{-2}	0.01	1.3
IODE IPSN[b]	1.7×10^{-3} Gy^{-1}	2×10^{-5}	0.5	2.1×10^{-6}	n.a.	n.a.

[a] changed from the first calculations

[b] The rate constants k_{14} and k_{-14} in IODE, used to represent $2IO_3 = I_2 + O_2$ are set to be the same as k_{13} and k_{-13}

[c] the user performed 5 calculations, varying both k_{13} and n to show code sensitivity

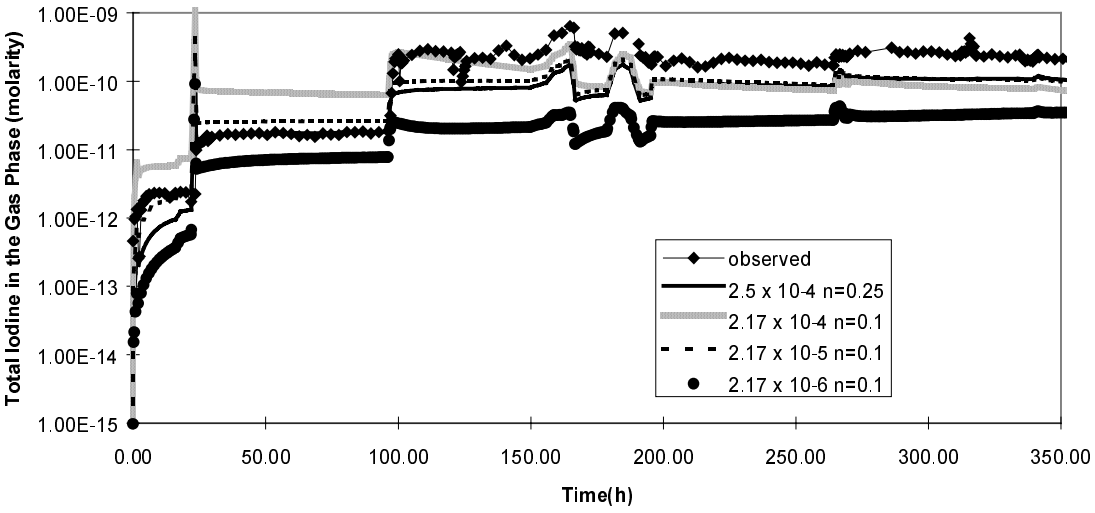

Figure 4. **The effect on gas phase iodine concentrations (as predicted by IODE) of the radiolytic rate constant k_{13}, and the value n.**

A Comparison of the mechanistic codes to the semi-empirical codes

The radiolysis models within the mechanistic codes such as LIRIC and MELCOR-outwardly appear very different from those within the semi-empirical codes. However, the basic structures of each type of model is sound. As can be seen from the discussion below, the numerous reaction schemes in a mechanistic model can be condensed into a few representative reactions (overall iodine oxidation and reduction reactions) in the semi-empirical models. The main difference between the mechanistic and semi-empirical codes is in the method of choosing the overall rate constants for the radiolytic oxidation of iodide, and reduction of molecular iodine. In the mechanistic codes, these rate constants are derived from solving a series of kinetic equations of fundamental chemical reaction whereas in the semi-empirical codes, the rate constants are extracted from simulation of experimental data.

LIRIC predicts that, in the absence of adsorption phenomena, the concentration of iodine species in the aqueous phase from irradiated solutions of CsI will reach a pseudo equilibrium concentration which is determined by the pH, dose-rate, and the concentration of impurities which can act as scavengers for water radiolysis products. An overall expression for the balance between oxidation of I^- (Reactions (8) and (9)) and reduction of I_2 (Reactions (11) and (12)) as calculated in LIRIC can be written as:

$$I^- (aq) \underset{k_{-22}}{\overset{k_{22}}{\longleftrightarrow}} I_2(aq) \qquad (22)$$

Reaction (22) is almost identical to Reaction (13) in the IODE/IMPAIR radiolysis model.

For the codes IMPAIR and IODE, a pseudo-equilibrium concentration of I_2 in the aqueous phase can be estimated from the forward (k_{13}) and reverse rates (k_{-13}), for the radiolytic oxidation of iodide and reduction of molecular iodine and the hydrolysis of I_2.[4] The pseudo-equilibrium concentrations of I_2 (aq) calculated at various pH values for several versions of IODE and IMPAIR are presented in Table 8 where they are compared to the steady-state I_2 (aq) concentrations predicted by LIRIC for the same conditions. The concentrations shown in Table 8 represent the maximum amount of I_2 which can be present in the aqueous phase for a given set of oxidation and reduction rate constants, because the calculation assumes that HOI disproportionation to IO_3^- is slow (as it is under all but the most basic of conditions). The concentrations were obtained by assuming no surface adsorption, and neglecting organic iodide formation or the presence of significant concentration of IO_3^-.

4. Note that thermal oxidation of iodide is ignored in this treatment, since the reactions are much too slow to compete with radiolytic formation.

Table 8. **Pseudo-equilibrium concentrations of $I_2(aq)$[a] as a function of pH as predicted by IODE[b], IMPAIR[c] and LIRIC[d] when adsorption is ignored**

	k_{13} **($(mol \cdot dm^{-3})^{-n}$**	k_{-13} **(s^{-1})**	n_1	$k_{13} \cdot D \cdot [H^+]^n$ at pH 5 **(s^{-1})**	Calculated $[I_2]^d$ in the aqueous phase as a function of pH **($mol \cdot dm^{-3}$)**		
					5	**7**	**9**
IMPAIR (PSI)	3.5×10^{-5} kGy^{-1}	2×10^{-7}	0.35	7.5×10^{-7}	3.7×10^{-5}	7.5×10^{-6}	1.5×10^{-6}
IMPAIR (SIEMENS)	2.3×10^{-4} kGy^{-1}	2×10^{-7}	0.1	1.0×10^{-4}	4.5×10^{-3}	2.9×10^{-3}	1.8×10^{-3}
IMPAIR (GRS)	2.3×10^{-4} kGy^{-1}	2×10^{-7}	0.4	3.2×10^{-6}	1.5×10^{-4}	1.7×10^{-5}	3.6×10^{-6}
IMPAIR (JAERI)	4×10^{-9}	1×10^{-15}	0.1	1.8×10^{-6}	n.a.[e]	n.a.[e]	n.a.[e]
IODE (IPSN)	1.7×10^{-3}	2×10^{-5}	0.5	8.4×10^{-6}	2.1×10^{-6}	1.4×10^{-7}	4×10^{-10}
IODE (CIEMAT)	2.5×10^{-4}	2×10^{-5}	0.25	5.4×10^{-6}	1.4×10^{-6}	3.1×10^{-7}	3.4×10^{-9}
IODE (NRIR)	0.1 Gy^{-1}	0	0.5	3.2×10^{-2}	n.a.[e]	n.a.[e]	n.a.[e]
LIRIC	n.a	n.a.	n.a.	n.a[d].	3.4×10^{-6}	2.7×10^{-7}	4.6×10^{-9}

[a] An equilibrium constant of 5.1×10^{-13} $mol^2 \cdot dm^{-6}$ was assumed for $I_2 + H_2O = HOI + H^+ + I^-$, and a dose-rate of 1.4 $kGy \cdot h^{-1}$ = 0.39 $Gy \cdot s^{-1}$ was used.

[b] Calculations for IODE: $\sum ([I_2(aq)] + [HOI(aq)]) = (k_{13} \cdot D(Gy \cdot s^{-1}) \cdot [H^+]^n \cdot [I^-(aq)]) / 2 \times k_{-13}$,

[c] Calculations for IMPAIR: $\sum ([I_2(aq)] + [HOI(aq)]) = (k_{13} \cdot D(kGy \cdot h^{-1}) \cdot [H^+]^n \cdot [I^-(aq)]) / (k_{-13})$

[d] In LIRIC, the rate of oxidation of iodide is ≈ 0.01 $mol \cdot dm^{-3} \cdot s^{-1}$. Reaction (8), $I^- + \cdot OH = I + \cdot OH^-$, has a rate constant of about 10^{10} $dm^{-3} \cdot mol^{-1} \cdot s^{-1}$. At iodide concentrations of 10^{-5} $mol \cdot dm^{-3}$, the $\cdot OH$ concentration is about 10^{-12} $mol \cdot dm^{-3}$. From the steady-state $I_2(aq)$ in this table, and the rate of Reaction (8), the overall reduction rate (which includes thermal reactions) can be estimated.

[e] IMPAIR (JAERI) and IODE (NRIR) do not predict a steady-state, since the value for k_{-13} is very small (JAERI) or 0 (NRIR).

Obtaining the correct pseudo-equilibrium I_2 concentrations at a given pH is the first step to deriving the correct rate constants. In addition, for a system such as the RTF experiment on which this ISP was based, mass transfer and surface adsorption need to be accounted for, and it is important to know the individual values for the rate constants such as k_{22} and k_{-22} rather than the just the psuedo-equilibrium constant k_{22}/k_{-22} (or $k_{13} \cdot D \cdot [H^+]^n / k_{-13}$). This is demonstrated by Reactions (22)-(24) which are simple representations of the processes of: radiolytic interconversion of iodine species; mass transfer across the aqueous/gas interface; and adsorption of molecular iodine on gas phase surfaces.

$$I^-(aq) \underset{k_{-22}}{\overset{k_{22}}{\longleftrightarrow}} I_2(aq) \qquad (22)$$

$$I_2(aq) \underset{k_{-23}}{\overset{k_{23}}{\longleftrightarrow}} I_2(g) \qquad (23)$$

$$I_2(g) \underset{k_{-24}}{\overset{k_{24}}{\longleftrightarrow}} I_2(ads) \qquad (24)$$

From Reactions (22)-(24) it can be seen that since processes such as mass transfer from the aqueous to the gas phase ($k_{23}[I_2(aq)]$), and reduction of I_2 in the aqueous phase, (k_{-22} $[I_2(aq)]$) compete with each other, the actual values for the rate constants corresponding to these processes must be well defined, and knowledge of the equilibrium constants or ratios k_{22}/k_{-22} alone is not sufficient to predict iodine volatility. For example, if the rate constant for mass transfer of $I_2(aq)$ from the aqueous to gas phase (k_{23}) is significantly larger than the rate of reduction of iodine in the aqueous phase (k_{-22}), the ratio of k_{22}/k_{23} would determine the concentration of iodine in the aqueous phase rather than the ratio k_{22}/k_{-22}. Thus the absolute value of k_{22} must be well established, as well as its value relative to k_{-22}. Establishing the absolute values of the rate constants becomes even more critical in more complex systems where other aqueous reactions of I_2 may occur (e.g. with organic impurities or Ag).

Despite the fact that the predicted steady-state concentrations reported in Table 8 cannot be directly applied to a "real" system, they are a useful starting point for comparison of radiolysis models, because they show the maximum amount of I_2 which could be generated in the aqueous phase by radiolysis. For example, a comparison between the steady-state $[I_2(aq)]$ concentrations calculated using LIRIC and IODE (as used by CIEMAT) show that very similar concentrations of I_2 are predicted at every pH. This is consistent with code calculations for the ISP exercise shown in Figure 5, in which the both the gas phase iodine concentrations, and the amount of iodine lost in the aqueous phase as predicted by these two codes agree reasonably well.[5] However, a comparison of the aqueous I_2 concentrations for LIRIC and IMPAIR (PSI) shows that the latter would predict several orders of magnitude more I_2 than would LIRIC. This is not borne out by the actual code calculations shown in Figure 5. The lower gas phase iodine concentrations observed in the IMPAIR (PSI) calculations as compared to LIRIC or IODE (CIEMAT) result from the rate of production of I_2 in the aqueous phase being considerably smaller for IMPAIR (PSI). Therefore, although the equilibrium concentration of I_2 as predicted by IMPAIR (PSI) is larger than for IODE (CIEMAT) or LIRIC, the rate at which the equilibrium is achieved is much slower. The rate of production of I_2 in IMPAIR is not sufficient to reproduce the experimental iodine behaviour, given that mass transfer and surface adsorption must also be considered.

5. Gas phase concentrations predicted by LIRIC and IODE in Figure 7 do not compare quite as well as the aqueous phase I_2 concentrations in Table 8 because as discussed, mass transfer and surface adsorption Reactions (23) and (24) are accounted for in the code calculations. Although the ratios k_{22}/k_{-22} in LIRIC and $k_{13} \cdot D \cdot [H^+]^n/(2 \times k_{-13})$ in IODE are similar, the individual rate constants are quite different.

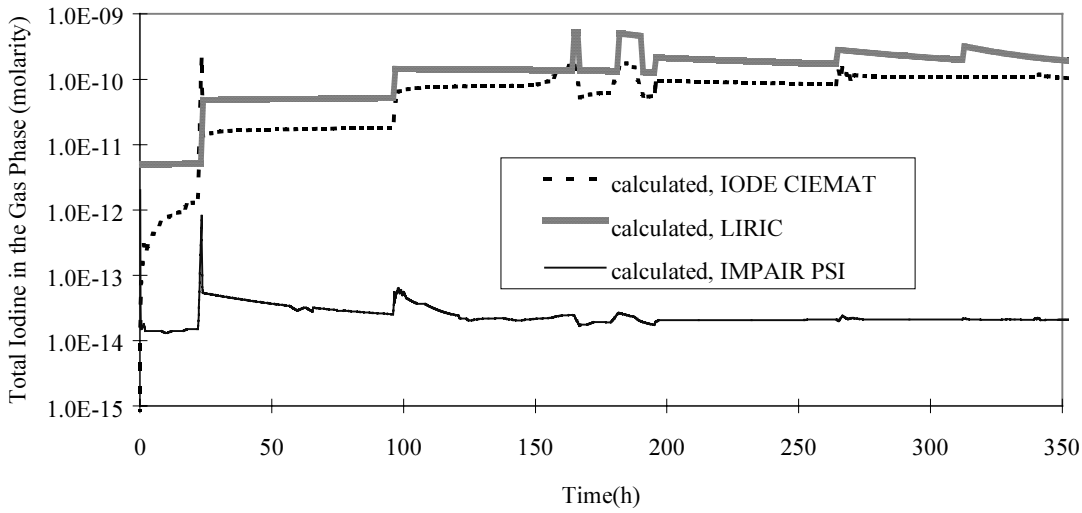

a)

b)

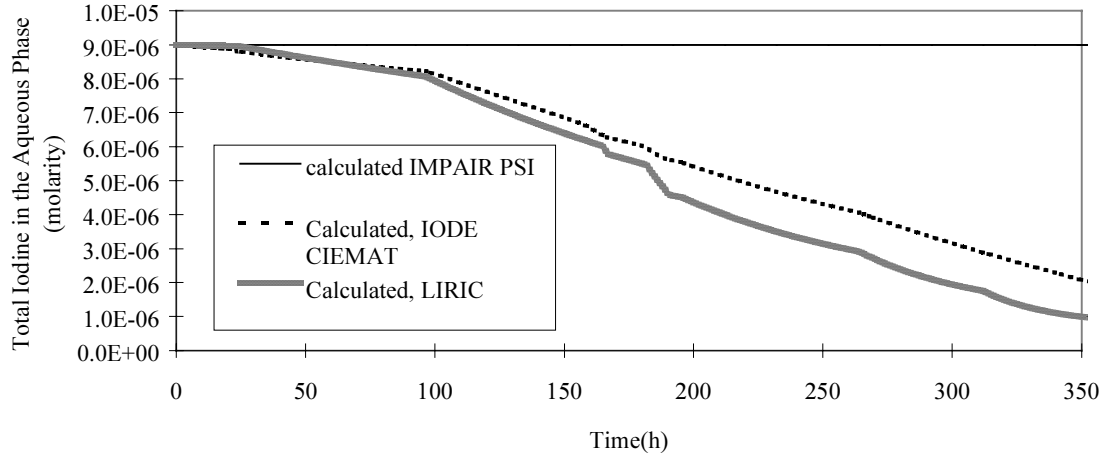

Figure 5. **A comparison of calculated results for Stage 1 from IMPAIR (PSI), IODE(CIEMAT) and LIRIC(AECL).**

A Comparison of the mechanistic codes

As demonstrated in Figure 6, results from MELCOR-I (Sandia) compare very well to those from LIRIC (AECL). This is not surprising, since the codes are very similar, and the rate constants for iodine reactions in the aqueous phase are very similar. The exception to the general good agreement between the two codes is at high pH values, an observation which has yet to be rationalised.

a)

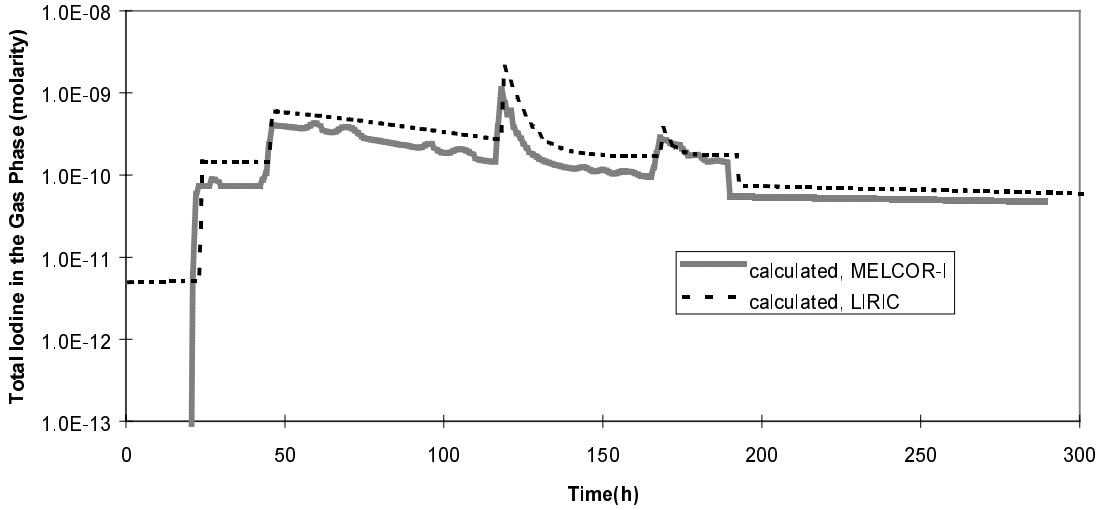

b)

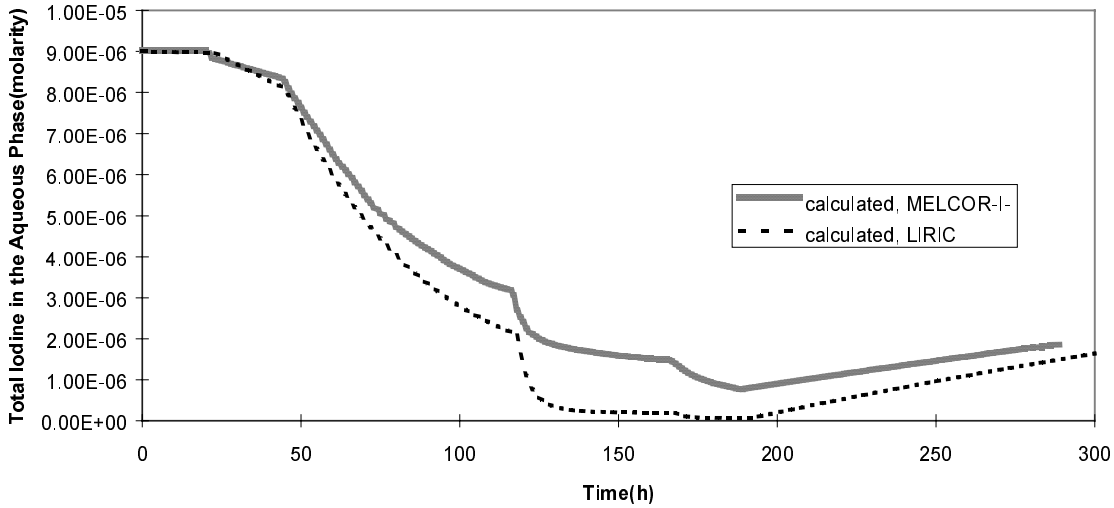

Figure 6. **A comparison of calculated results for Stage 2 from MELCOR-I (Sandia), and LIRIC (AECL).**

5.3 Summary

The above comparison of the codes used by the various participants for this exercise demonstrates three important points regarding the nature and the performance of the codes.

1) The comparison illustrates that both the mechanistic and semi-empirical modelling approaches for pool chemistry are fundamentally sound. Whereas the mechanistic codes are more flexible by virtue of their ability to cover a wider range of conditions (without changing input rate constants), encapsulating the series of complex equations into a smaller number of equilibrium reactions results in simple radiolysis model which is easier to use.

The simpler codes have the potential to reproduce experimental data remarkably well, (cf. NRIR's and CIEMAT's IODE calculations).

2) The key ingredient for a successful semi-empirical radiolysis model is in developing a rational process for defining its input rate constants so that it maintains the flexibility of the more complex mechanistic models. This second point which was demonstrated by the comparison is that it is very difficult to define rate constants for the simple radiolysis models such that these models can be used with confidence over a range of different conditions. This difficulty is the reason why many of the calculations (which used radiolysis rate constants derived from data obtained at higher temperature) did not reproduce the experimental results adequately.

3) Finally, the comparison has shown that an important criteria for the choice of rate constants is that these rate constants be defendable. The rate constants must be within the boundaries set by physical limitations, and they must be chosen such that they do not impose unrealistic physical limitations on the code.

6. CONCLUSIONS

The experiments on which this ISP exercise was based were performed under controlled and very limited conditions. They were chosen as a starting point for evaluation of the various iodine behaviour codes because of their simplicity, in the hope that the very basic components of each code could be compared. This objective was realised. From this simple exercise a number of important points regarding the iodine behaviour codes were demonstrated. These are summarised below:

1) The ISP exercise demonstrated that all the codes were capable of giving a reasonable reproduction of test results based on the established criteria previously discussed (see Section 5.0), given the appropriate parameters, some of which are default values, and others which are user defined kinetic rate constants. It also demonstrated that choice of these code parameters is key to code performance. These code parameters, in order of least to most important for these experiment are:

   - mass/transfer coefficients;
   - adsorption/desorption rate constants;
   - radiolysis rate constants.

For the mechanistic codes, no user defined rate constants are required for the radiolysis models. The assumption inherent in the mechanistic approach to modelling aqueous radiolytic reactions is that if the separate components of the radiolysis model (e.g. water radiolysis, radiolytic reactions of iodine species) have been demonstrated to be valid over a wide range of conditions, and the relationship between the components (e.g. the effect of dose-rate, water radiolysis product concentration, temperature, and pH on iodine behavior) is well understood, the entire radiolysis model should be valid over the same range of conditions. This requires, of course, that mechanisms within the model are correct, and the rate constants for individual reactions are well defined. For IMPAIR and IODE, radiolysis rate constants are considered to be default parameters, however, development of these codes is ongoing, thus default parameters differed between users.

2) The sensitivity of code performance to user defined rate constants, as demonstrated by the wide spread in the calculation results from this exercise is a reminder that one should exercise caution when using code calculations as predictive or interpretive tools.

   - The appropriate choice of kinetic rate constants for modelling depends upon the conditions for which the code is used and knowing which kinetic parameters to use for these conditions. This necessitates either finding the optimum parameters for data which covers the entire range of the conditions of interest, or demonstrating that the kinetic parameters can be extrapolated from data obtained under more limited conditions. The ISP exercise provided an opportunity for each of the participants to critically evaluate the pH dependence of their iodine radiolysis models as a function of kinetic parameters. As a result, serious consideration is being given by some participants to changing portions of their models.

   - Evaluation of code performance using an RTF test performed at 25°C is not necessarily applicable to its performance at the higher temperatures more relevant to severe accident scenarios. In fact, IODE and IMPAIR have not been validated at lower temperatures, and this is one reason why there was a difference in calculation results between various users. However the exercise provides a starting point for establishing the range of kinetic parameters required for modelling iodine behaviour.

In conclusion, the exercise demonstrated that all the iodine behaviour codes could adequately reproduce the experimental results which were chosen for this exercise. However, it also demonstrated that, for the most part, the iodine behaviour codes are at the developmental stage where code performance is still extremely reliant upon the availability of suitable data, and the judicious choice of code kinetic parameters. If the ultimate purpose of the iodine behaviour codes is for predicting iodine volatility under postulated reactor accident conditions, conditions which may be very different from the tested range of applicability of the codes, it is important that the developers and users of these codes make appropriate choices for these code parameters. It is also important to provide transparent justification for these choices.

7. RECOMMENDATIONS

As outlined in the objective, this ISP exercise was chosen as a starting point for code comparisons in the hope that the very basic components of each code could be compared. This was achieved in terms of establishing that iodine volatility as a function of pH can be well reproduced by all codes. Other aspects of applicability of the codes, such as predicting pH changes, modelling the effects of temperature on adsorption behaviour under accident conditions etc., were not examined. Therefore, the possibility of doing additional ISP exercises was discussed. Two sets of exercises were proposed, a set of parametric studies, and two integrated experiments.

7.1 Parametric calculations

The parametric calculations were seen as desirable to allow the code users to evaluate the sensitivity of their codes to boundary conditions such as pH, dose-rate, temperature, and initial I^- concentration. A range of conditions of interest for parametric calculations was established. The ranges defined were:

pH 3 - 10
temp. 25 - 150 °C

dose-rate 100 - 0.1 kGy·h^{-1}, and
initial [I^-] 10^{-7} - 10^{-3} moles·dm^{-3}.

A matrix for parametric studies covering some of this range has been proposed.

T (°C)	**pH***	**[I^-] (moles·dm^{-3})**	**dose-rate (kGy·h^{-1})**
130	9-7-5	10^{-4}	10
90	9-7-5	10^{-5}	1
50	9-7-5	10^{-6}	0.1
130	9-7-5	10^{-6}	1

* three distinct stages each at a constant pH.

Total distribution of iodine between the three phases (gas, aqueous and surfaces) will be calculated with speciation of iodine an optional exercise. Aqueous, gas volumes, interfacial surfaces areas and painted surface areas will be decided on at a later date but will be representative of containment. Both condensing and non-condensing conditions will be examined. The presence of Ag, and the initial speciation of iodine (0% and 3% I_2 initially released into the atmosphere, with the remainder in the form of I^-) will also be considered.

Although the number of cases to be calculated is fairly large the amount of time required for each participant to perform these calculations is anticipated to be only 3-4 weeks.

7.2 Blind post-test calculations

For the integrated experiments, data from the RTF and Caiman facilities were examined and the participants stated a wish for modelling organic iodine formation, pH changes in unbuffered solutions relevant to accident conditions and iodine radiolysis at temperatures higher than 25°C. Two integrated experiments, one from each facility will be used.

The most appropriate RTF experiment for the exercise was performed in an Amerlock 400 (epoxy-coated) vessel, at 60°C and with a dose-rate of 0.6 kGy h^{-1} (0.06 MRad h^{-1}). The experiment was performed in two stages. The first stage was initiated at pH 10 in the absence of added CsI. The pH was uncontrolled, and organic compounds leaching out of the painted surface, and their radiolytic decomposition products, were identified and quantified, while monitoring the changes in pH induced by this radiolytic decomposition.. In the second stage of the experiment, performed with a fresh charge of water, the pH was adjusted to 10 and ^{131}I trace labelled CsI was added. The pH was controlled at 10 for 72 hours, and then pH control was removed. After 285 hours the pH was again adjusted to 10, and controlled for the remainder of the experiment, which lasted 335 hours. The total iodine concentrations in the gas and aqueous phase, and speciation of iodine in both phases were monitored throughout the second stage of the test. In addition, the concentration of several organic species in both phases were monitored.

A table of possible choices for the Caiman facility experiment are listed on the next page.

CAIMAN EXPERIMENTS

Initial experimental conditions review

test number	Species and initial concentrations	pH	Sump temperature	gas temperature/pressure	dose rate	paint coupons location
Caiman97/02	I^- : 10^{-5} mol·dm^{-3} I_2 : 0 mol·dm^{-3}	5 (1)	90 °C	110 °C 2.9 bar	0.3 MRad h^{-1}*	sump and gas
Caiman97/04 (4)	I^-:1.5×10^{-5} mol·dm^{-3} I_2 : 0 mol·dm^{-3}	5 (for 48 h) (1) 9 (for 24 h) (1)	121 °C	134 °C 3.7 bar	0.3 MRad h^{-1}*	sump and gas (2)
Caiman97/06 (4)	I^-: 1.5×10^{-5} mol·dm^{-3} I_2 : 0 mol·dm^{-3}	9 (for 24 h) (1) 5 (for 48 h) (1)	121 °C	134 °C 3.7 bar	0.3 MRad h^{-1}*	sump and gas (2)
Caiman98/01 (3) (4)	I^-: 1.5×10^{-5} mol·dm^{-3} I_2 : 0 mol·dm^{-3}	5	130 °C	70 °C 3.7 bar	0.3 MRad h^{-1}*	sump and gas

(1) : uncontrolled pH during the experiment (no LiOH and H_2SO_4 addition)

(2) : gaseous painted surface cooled down to 117 °C to allow steam condensation onto this surface

(3) : the main feature of the Caiman 98/01 test is a high evaporation rate to make molecular and organic iodine transfer easier from the sump to the gas phase.

(4) : for these three tests, in-gas iodine measurements aren't reliable :

- Caiman 97/04 : heating system failed early in the May-pack loop leading to high steam condensation onto the May-pack media.
- Caiman 97/06 and Caiman 98/01 : the flowmeter was damaged, preventing gas mixture from circulating into the May-pack loop.The painted coupon insulated in the gas phase allows to get trends about gaseous molecular iodine concentration

* remark: the dose rate, provided by a ^{60}Co source, is now significantly lower than the initial value of 0.3 Mrad/h (the half-life for decay of ^{60}Co is around five years). It would be better to consider a 0.1 Mrad/h dose rate for the tests performed during the last year (a report on the dose rate map in the sump has been issued)

REFERENCES

1. WREN, J.C., GLOWA, G.A., and BALL, J.M (1996), Modelling Iodine Behaviour Using LIRIC 3.0, Proceedings of the Fourth CSNI Workshop on the Chemistry of Iodine in Reactor Safety, Wurenlingen, Switzerland.

2. SCHWARZENBACH, R.P., GSCHWEND, P.M. and IMBODEN, D.M (1993), "Environmental Organic Chemistry", John Wiley and Sons Inc. Toronto.

3. JACQUEMAIN, D., IPSN, personal communication.